



HAL
open science

On the dual behaviour of water in octanol-rich aqueous n-octanol mixtures: an x-ray scattering and computer simulation study

Martina Požar, Jennifer Bolle, Christian Sternemann, Aurélien Perera,
Susanne Dogan-Surmeier, Michael Paulus, Eric Schneider

► To cite this version:

Martina Požar, Jennifer Bolle, Christian Sternemann, Aurélien Perera, Susanne Dogan-Surmeier, et al.. On the dual behaviour of water in octanol-rich aqueous n-octanol mixtures: an x-ray scattering and computer simulation study. 2023. hal-04258497

HAL Id: hal-04258497

<https://hal.science/hal-04258497>

Preprint submitted on 25 Oct 2023

HAL is a multi-disciplinary open access archive for the deposit and dissemination of scientific research documents, whether they are published or not. The documents may come from teaching and research institutions in France or abroad, or from public or private research centers.

L'archive ouverte pluridisciplinaire **HAL**, est destinée au dépôt et à la diffusion de documents scientifiques de niveau recherche, publiés ou non, émanant des établissements d'enseignement et de recherche français ou étrangers, des laboratoires publics ou privés.

On the dual behaviour of water in octanol-rich aqueous n-octanol mixtures: an x-ray scattering and computer simulation study

Martina Požar¹, Jennifer Bolle², Susanne Dogan-Surmeier²,
Eric Schneider², Michael Paulus², Christian Sternemann^{2*} and
Aurélien Perera^{3 †}

September 22, 2023

¹University of Split, Faculty of Science, Ruđera Boškovića 33, 21000 Split, Croatia

²

, Technische Universität Dortmund, D-44221 Dortmund, Germany

³Sorbonne Université, Laboratoire de Physique Théorique de la Matière Condensée (UMR CNRS 7600), 4 Place Jussieu, F75252, Paris cedex 05, France.

Abstract

Aqueous *n*-octanol ($n = 1, 2, 3, 4$) mixtures from the octanol rich side are studied by x-ray scattering and computer simulation, with focus on structural changes, particularly in what concerns the hydration of the hydroxyl-group aggregated chain-like structures, under the influence of various branching of the alkyl tails. Previous studies have indicated that hydroxyl-group chain-cluster formation is hindered in proportion to the branching number. Here, water mole-fractions up to $x = 0.2$ are examined, i.e. up to the miscibility limit. It is found that water molecules within the hydroxyl-chain domains, participate to the chain formations in different manner for the 1-octanol and the branched octanols. The hydration of the octanol hydroxyl chains is confirmed by the shifting of the scattering pre-peak to low momentum transfer both from measured and simulated x-ray scattering intensities, which corresponds to an increased size of the clusters. Experimental x-ray scattering amplitudes are seen to

*christian.sternemann@tu-dortmund.de

†aup@lptmc.jussieu.fr

increase with increasing water content for 1-octanol, while this trend is reversed in all branched octanols, with the amplitudes decreasing with the increase of branching number. Conjecturing that the amplitudes of pre-peaks are related to the density of corresponding aggregates, these results are interpreted as water breaking large OH hydroxyl chains in 1-octanol, hence increasing the density of aggregates, while enhancing hydroxyl aggregates in branched alcohols by inserting itself into the OH chains. Hence, water acts as a structure maker or breaker in inverse proportion to the hindering of OH hydroxyl chain structures arising from the topology of the alkyl tails (branched or not).

1 Introduction

It is well known that alcohols are characterized by the chain-like association of the OH hydroxyl groups, which give rise to a scattering pre-peak in radiation scattering experiments [1, 2, 3, 4, 5, 6, 7, 8, 9, 10, 11, 12, 13, 14], and also from scattering intensities calculated from computer simulations [15, 16, 17, 18, 19, 20, 21, 22, 23]. What is perhaps less known is the influence of the alkyl tail parts, both in their length and their branching possibilities. The n -octanols are ideal case for this study, because the alkyl tails are reasonably long, and 4 branching conditions are possible, as illustrated in Fig. 1.

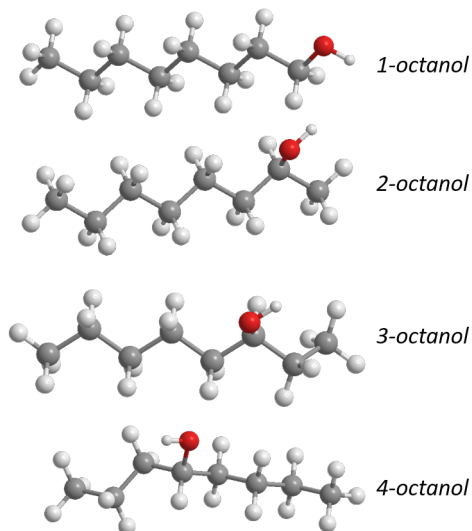


Figure 1: Octanol molecules branching. The molecules were visualised using ChemDraw (Chem3D; PerkinElmer Informatics).

Alcohols beyond propanol are no more fully miscible in water, indicating that alkyl chain lengths beyond 4 are already too hydrophobic for water to accommodate. Indeed, the volume ratio of charged (hydroxyl head groups) and

uncharged (alkyl tails) decrease as $1/m$, where m is the alkyl tail length in terms of methyl/methylene units. For octanol, the volume of hydrophobic units is 8-fold that of the hydrophilic units, twice that of 1-propanol. As water is added to neat alcohols, it is initially expected that it would associate to the hydroxyl groups, which are already grouped in chains. But this Coulomb empathetic association is not expected to hold when the water content is increased. For small alcohols, micro-segregation of the alcohol and water is observed, with the help of water-hydroxyl group proximity[24]. Also, chaining of the hydroxyl groups is suppressed at high water content. This crossover from monomeric to chain formation is conditioned by the alkyl chain length and bulkiness, and cannot occur without a full phase separation beyond $m = 4$ [25]. This implies that the micro-segregation picture of miscible small alcohols is lost with longer ones. Therefore, it is interesting to examine how water affects the OH chain formation before the breaking point, and also how the alkyl tail “bath” influences water location.

The experimental x-ray spectra can be intuitively interpreted in terms of underlying structure formation, but only to some extent. Computer simulations provide a microscopic picture through the statistical analysis of many possible molecular configurations. However, simulations come with their own load of problems, the most important being the use of model molecular force fields, such that the systems studied do not quite correspond to the experimental ones. Interpreting fine details differences in par with the intuitive ideas provided by the experimental spectra is a difficult exercise, possibly there is no guarantee that a unique interpretation is possible. This is confirmed by previous studies of 1-octanol-water mixtures.

The 1993 paper of Franks *et al.* [9] used a modified hard sphere model to fit the hydroxyl group aggregates of neat 1-octanol to a spherical core, thus providing a perfect fit of the pre-peak shape. The 2002 paper by McCallum and Tieleman [26] concerns computer simulations of neat and hydrated 1-octanol. The snapshots from computer simulation show very clearly that the OH hydroxyl groups form chains and not spheres, hence proving the model of Franks and coworkers incorrect, despite the impeccable fit of the pre-peak. The same simulation shows that water tends to insert within the hydroxyl chains, and that the pre-peak amplitude increases with water concentration. Finally, the 2006 paper by Chen and Siepmann [18] is a Monte Carlo simulation study of dry and wet octanol with different force fields. The authors confirm the formation of OH chains, with insertion of water inside the chains. In addition, they report that water tends to distribute itself more on very long neat 1-octanol chains than short ones, hence diminishing the number of pure 1-octanol long chains. This last trend is equally observed by us, but with the added interpretation that water tends in fact in breaking OH chains, thus acting as a structure breaker, a conclusion that is not reached by this earlier study. Other experimental studies of aqueous n-octanol, are mostly limited to 1-octanol, and do not provide very accurate microscopic pictures. Several types of studies have been performed, such as the thermodynamic studies [27, 28], spectroscopic studies [29, 30], or interfacial descriptions through simulation methods [31].

The pathway we choose in this paper is the following. The various octanol alcohols are systems ordered at microscopic level, in the sense that hydroxyl groups form various types of chains. Adding water to these alcohols will eventually lead to full demixing already at water concentration as low as $x \approx 0.25$. Hence, studying the mixing of water with these alcohols is akin to studying precursor demixing conditions. On the other hand, it seems intuitively clear that water molecules will preferably stay in the vicinity of the hydrophilic hydroxyl chain groups, and tend to perturb these chains. Eventually, this perturbation will break the stability of the system, which will prefer to phase separate by segregating the water molecules into pockets separated from the ordered octanols. Computer simulation can provide some support to how this happens. What we find is that water plays both the role of structure maker and breaker, depending on if the octanols are branched or not. In what follows, we try explain how the various microscopic indicators from the simulation can help support this picture.

2 Experimental and simulation details

2.1 Experimental

Pure octanol isomers and octanol/water mixtures were studied by x-ray diffraction at 293 K. We purchased 1-octanol (purity > 99.7%), 2-octanol (purity > 99.5%), 3-octanol (purity > 99.5%) and 4-octanol (purity > 97%) from Sigma Aldrich and used them without further treatment. Mixtures were produced using MilliQ water. The solubility of water in 1-octanol and 2-octanol is small and even smaller for the highly branched octanols. Hence we were able to study 1- and 2-octanol for water molar fractions x up to 0.2 while 3- and 4-octanol were investigated up to $x = 0.1$ to avoid demixing. The pure alcohols and water-alcohol mixtures were filled into borosilicate capillaries with 0.01 mm wall thickness for the diffraction study.

The x-ray diffraction measurements were performed at the bending magnet beamline BL2 of the synchrotron radiation source DELTA (Dortmund, Germany) [32]. We used a multilayer monochromator providing an incident energy of 10.87 keV with a bandpass of about 10^{-2} and a beamsize of $0.5 \times 0.5 \text{ mm}^2$. The diffraction images were measured with a MAR345 image plate detector. LaB₆ was used a calibration standard. The 2D diffraction images were converted to diffraction patterns with the software package Fit2D [33]. Finally, the air scattering and scattering from capillary was subtracted and the data were normalized to the integrated intensity of the calculated diffraction patterns of the pure octanols in the wave-vector transfer k -range between 0.2 and 2.3 \AA^{-1}

2.2 Simulations

Molecular dynamics simulations of the octanol-water mixtures were conducted in the Gromacs program package [34]. The initial configurations of 2048 molecules

for all systems were created with Packmol [35]. These initial configurations were first energy minimized and then equilibrated for 5 ns. Finally, production runs of 5 ns were performed during which at least 2000 configurations were gathered. The simulations were done in the NpT ensemble at $T = 300$ K and $p = 1$ bar. The temperature was maintained with the v-rescale thermostat [36], whereas the Parrinello-Rahman barostat [37, 38] was utilized to keep the pressure constant. The temperature algorithm had a time constant of 0.2 ps and the pressure algorithm was set at 2 ps.

The leap-frog algorithm [39] was used as the integration algorithm, at every time-step of 2 fs. The short-range interactions were calculated within the 1.5 nm cut-off radius. The long-range electrostatics were handled with the PME method [40] and the constraints with the LINCS algorithm [41]. The forcefield of choice for the octanols was the OPLS-UA [42], while the SPC/e model was used for water [43].

3 Comparison of measured and calculated x-ray intensities

3.1 Experimental data and two conjectures

The x-ray scattering experiments are summarized in Fig.2, for different branching of the octanol and different water mole fractions of $x = 0.07, 0.1, 0.2$ for 1-octanol, $x = 0.045, 0.15, 0.2$ for 2-octanol, $x = 0.07, 0.1$ for 3-octanol, and $x = 0.06, 0.1$ for 4-octanol.

In the discussion below, we pay attention to two principal features: the amplitudes and the k -positions of the main peak (around $k \approx 1.4 \text{ \AA}^{-1}$) and the pre-peak (in the k -range $0.4 - 0.6 \text{ \AA}^{-1}$) and their changes with water insertion. We use two conjectures: the k -positions are related to objects size and the amplitudes are related to the density of the objects. By object, we mean the atoms or atomic groups (such as the methyl group) inside molecules and the clusters of the hydroxyl head groups when it concerns the main peak and pre-peak, respectively. By object size we mean that defined through the inter-object contact, such as for instance defined by the minimum of the inter-particle interaction.

In a previous work on octanols[23], we have shown that both conjectures were fully consistent with the temperature dependence of $I(k)$, both for the main peak and the pre-peak. Essentially, we found that both the amplitudes of the main peak and pre-peak increased with the decrease of temperature, a trend which is consistent with the densification of liquids upon cooling since objects tend to occupy less volume. Similarly, the increase of peaks' k -values, were shown to be consistent with a tightening of contact due to increased interactions due to the Boltzmann factor $k_B T$. In the present case, because of the very small effects of water insertion on $I(k)$, the conjecture is less obvious, particularly for the pre-peak.

These conjectures make sense for the main peak, since it concerns atomic

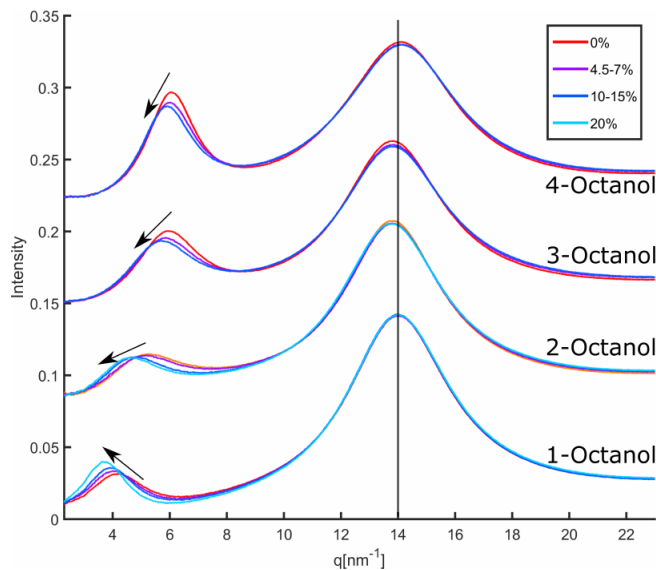


Figure 2: X-ray scattering intensities of n -octanol-water mixtures with $n=1, 2, 3, 4$ with different mole fractions of water. The data are normalized to the integrated scattering intensities of the pure octanols from the simulations. The arrows are guides to the eyes.

groups which are well defined by the interaction force field. For the octanols considered here, the methylene groups of size $\sigma_m \approx 3.75\text{\AA}$ are dominating the system in a ratio 8/10. Hence, the scattering main peak is positioned at $k = 2\pi/\sigma_m \approx 1.67\text{\AA}^{-1}$, which confirms part of the stated conjecture. However, the experimental main peak positions around 1.4\AA^{-1} indicate a somehow larger effective diameter of about 4.5\AA . Concerning the amplitudes of the main peak, they are found to be nearly insensitive to the addition of water, since the density change is so small.

For the pre-peak however, the conjectures are important to explain the observed changes, highlighted by the arrows in Fig.2, particularly in what concerns the amplitudes. This is because clusters are entities with a distribution of sizes and densities. While all isomers exhibit a decreasing pre-peak position k_{PP} with increasing water addition, their amplitudes vary in a very different way. For 1-octanol the pre-peak intensity increases with higher water content. For 3- and 4-octanol this trend is reversed. Latter is observed also for 2-octanol but to a lesser extent.

3.2 Data from simulations

The calculated diffraction intensities based on the molecular dynamics simulations are presented in Fig.3. We simulated octanol-water mixtures for molar

fractions of $x = 0.02, 0.05, 0.1, 0.2$ for 1 and 2-octanol and $x = 0.02, 0.05, 0.1, 0.15$ for 3 and 4-octanol. The most notable facts are the positions of the main peaks and pre-peaks, as well as both their amplitudes, which follow the same patterns as those of the experimental data in Fig.2, except for pure 3-octanol and to a lesser extent pure 4-octanol. Similarly to the experimental data, the main peak does not change significantly with addition of water. The OPLS force field gives the methylene CH_2 atom size around $\sigma \approx 3.75\text{\AA}$ which corresponds to the main peak positions $k_{MP}^{(calculated)} \approx 1.67\text{\AA}^{-1}$, enforcing the interpretation of the peaks in terms of mean scattering object size.

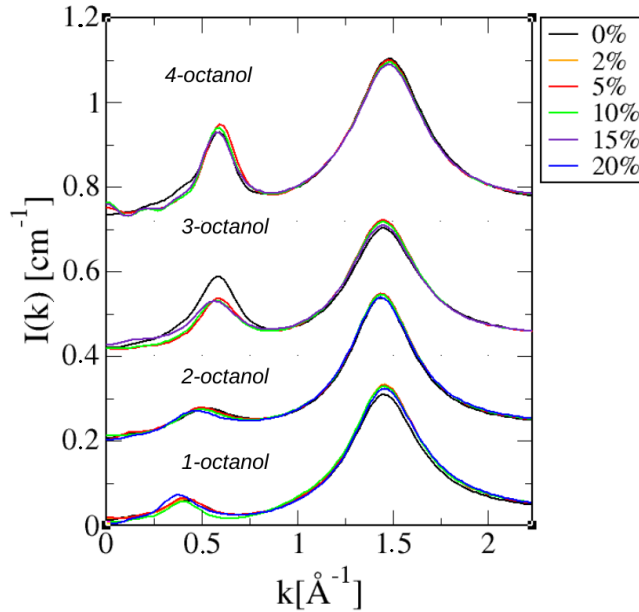


Figure 3: X-ray scattering intensities of n -octanol-water mixtures with $n = 1, 2, 3, 4$ as calculated from computer simulations.

Interestingly, the pre-peak behavior of the simulated intensities resembles surprisingly well to the findings from the experiment. Except for dry 3-octanol and 4-octanol, we observe in the simulation a shift of the pre-peak to lower k . The variation of the pre-peak intensity is most obvious if the lowest (2%) and highest (15% – 20%) water concentrations are considered: For 1-octanol the intensity increases while it decreases for all branched octanols with addition of water. Overall we see a rather good agreement between experiment and simulation which allows us to look deeper into the structural details analyzing the simulated snapshots, atom-atom structure factors, and correlation functions. The case of 4-octanol is also examined below. There are obvious cases of disagreements, such as the intensity of the pre-peak of dry 3-octanol being much higher than for the wet ones. Latter is observed in opposite but to a lesser

extend for 4-octanol. Surprisingly, these trends are reproducible from one run to another, even when started from different initial conditions. We get back to this later, when examining microscopic details from simulations.

In order to better interpret these scattering intensities, we recall the Debye expression relating the scattering intensity $I(k)$ to the *total* atom-atom structure factors [44, 45, 22]:

$$I(k) \approx \sum_{i,j} \sum_{a_i,b_j} \sqrt{x_i x_j} f_{a_i}(k) f_{b_j}(k) S_{a_i b_j}^{(T)}(k) \quad (1)$$

where sums run on molecular species with index i and j , as well as the atoms a_i and b_j belonging to the respective molecules, ρ is the total number density, $x_{i,j}$ is the mole fraction of species i, j , $f_{a_i}(k), f_{b_j}(k)$ are the form factors of atoms a_i, b_j , and

$$S_{a_i b_j}^{(T)}(k) = W_{a_i b_i}(k) \delta_{ij} + \rho \sqrt{x_i x_j} \int d\mathbf{r} \exp(i\mathbf{k} \cdot \mathbf{r}) [g_{a_i b_j}(r) - 1] \quad (2)$$

where $W_{a_i b_i}(k)$ is the Fourier transform of the intra-molecular correlation function [22] for species i (there are no intra-molecular correlations for cross molecular species, hence the Kronecker delta δ_{ij} , and $g_{a_i b_j}(r)$ the pair correlation function between the atoms a_i and b_j).

The interpretation of the intensity of the pre-peak in terms of aggregate density is not obvious to justify from theoretical grounds. Indeed, the pre-peak is the result of cancellations of positive atom-atom correlation pre-peaks and negative atom-atom correlation anti-peaks. Fig.SI-1 in the Supplementary Information (SI) shows all the structure factors for 1-octanol and highlights typical ones, where the pre-peaks and anti-peaks are visible. The origin of these atom-atom pre-peaks and atomic peaks is related to charge order, and ultimately refer to the local arrangements of the charged molecular groups with respect to the uncharged ones. Indeed, the correlations between the charged groups tend to produce positive atom-atom pre-peaks, while the negative anti-peaks come from the charged-uncharged cross correlations. For example, the pre-peak for the case of methanol is weaker (almost a shoulder), while that of ethanol and higher alcohols is more pronounced and higher in amplitude[22]. From these information, we can conclude that the intensity of the pre-peak reflect the density of the charged groups in the midst of uncharged ones, namely that of the hydroxyl group clusters in the “bath” of alkyl tails. This interpretation had been tested in the case of pure branched octanols [23] and could be put to the test in the present case.

The main peak is seen to be quite insensitive to the addition of water, which is fully consistent with the picture that water essentially contributes to the aggregates through the cluster pre-peak. Indeed, the main peak reflects the mean atom size, which is dominantly that of the methyl/methylene groups (around 4 Å for the OPLS united atom model [42]). The interpretation of the pre-peak positions in Ref. [23], was in terms of aggregate sizes in condition where the branching of the alkyl tail hinders the chain formation of the hydroxyl groups.

Indeed, the shift of the pre-peak positions towards larger k values consistently indicates a smaller size of the hydroxyl aggregates. For the case of 1-octanol, the addition of water shifts the pre-peak to smaller k -values, again confirming that the water molecules tend to increase the size of the hydroxyl head groups by sitting between them. The same trend is equally seen for the branched octanols, which is more or less the expected result.

Turning to the pre-peak intensity, we note that they show a highly unexpected behaviour. For 1-octanol, the intensity of the pre-peak increases with addition of water, while it appears to decrease for the branched ones. On the other hands, the intensities increase systematically when going from 1-octanol to 4-octanol. This is perfectly consistent with the interpretation of the intensity of the pre-peak as the density of the aggregates. Indeed, if the aggregates become smaller with branching, since both the number of OH groups and CH groups is exactly the same for all octanols, it clearly means that the number of smaller OH aggregates must necessarily increase with the reduction of the chain size.

If we reason in terms of associating the pre-peak intensity to the density of hydroxyl group aggregates, independently of their sizes, the case of 1-octanol suggests that the number of chains increases with water addition. This means that the insertion of more and more water tends to destabilize the hydroxyl head group chains, and these break in smaller ones, with water replacing the hydroxyl groups. The decrease of the amplitude for the branched alcohols is interpreted as water allowing more hydroxyl groups to gather, hence increasing the aggregate sizes, but decreasing their density. In other words, in the case of the branched octanol, water acts as an aggregate cement, while it acts as an aggregate disruptor for the 1-octanol.

4 Microscopic details from computer simulations

The most straightforward approach is to analyse the cluster distributions obtained from the computer simulations, which we provide in the next subsection. The analysis of the atom-atom pair correlation functions and related structure factors in a second subsection, help better understand what happens at atomic level.

4.1 Cluster analysis

Fig. 4 shows the compared oxygen cluster distributions between 1-octanol and 4-octanol, both in neat and maximum hydrated conditions, which is 20% for 1-octanol and 15% for 4-octanol. The most apparent feature is the cluster peak around cluster size 5, which is common to all curves. Previous works have demonstrated that cluster size 5 seems to be a magic number common to all mono-ols [22]. Comparing first the neat 1-octanol (open circles) and neat 4-octanol (filled circles) distributions, we see that 4-octanol has less small and large clusters than 1-octanol, but most mean size clusters, between 4 and 6. This indicates that the cluster size distribution is more polydispersed for 1-

octanol than 4-octanol, and in particular that there are more large clusters in 1-octanol than 4-octanol. These conclusion were previously reached in our work [23].

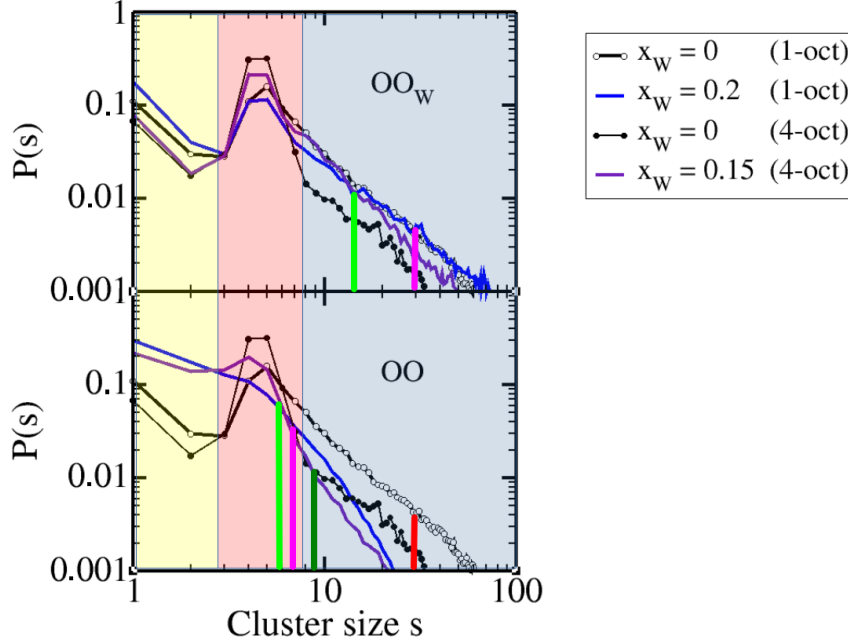


Figure 4: Oxygen atom clusters size distributions for 1-octanol and 4-octanol, both in neat and maximum hydration conditions. Upper panel for the cross oxygen OO_w clusters and lower panel for octanol OO clusters. The pure n-octanol curves (open circles for 1-octanol and filled circles for 4-octanol) are reproduce in both panels to facilitate the discussion. The coloured areas are discussed in the text. The thick colored vertical lines refer to the mean size of clusters, with the following color conventions: red and magenta for neat and aqueous 1-octanol, respectively, dark and pale green for neat and aqueous 4-octanol, respectively.

There are 3 colored parts to focus on, the small cluster sizes, under 3 units (colored in pale yellow), just below the peak, the peak region itself coloured in pale red), from 4 to 6-7, and the tail part, above 7 units (coloured in blue). When water is added to near saturation, if we compare with neat octanol cluster distributions, the small size clusters generally increase, but spectacularly so for neat OO clusters than mixed OO_w ones. The peak is generally diminished, but nearly vanishing for the case of 1-octanol OO clusters. Concerning the tail part, there are 2 distinct behaviour: for the mixed OO_w clusters, the distribution looks more like that of neat 1-octanol, while the OO cluster look more like neat 4-octanol. Putting all these results together, when water is added, the OO

clusters are pushed towards smaller sizes, while the mixed OO_w clusters tend to be larger.

For 1-octanol, the initial OO clusters have been replaced by OO_w clusters. Since the initial OO clusters were rather large ones, it means that water has broken them by inserting into them. This means that the total number of clusters has increased (see OO_w and OO distributions), which is compatible with the increase of the pre-peak amplitude. These interpretations are compatible with water playing the role of a structure breaker in the case of 1-octanol.

In the case of 4-octanol, the large OO cluster size remains more or less the same, but the small cluster size has increased and become more polydisperse, nearly losing the clear OO cluster peak. Conversely, the number of large OO_w clusters have increased. Clearly, water has acted as a structure maker in the case of 4-octanol.

An important point to consider is the fact that these cluster distributions give only probabilities of sizes, and not the number of clusters of given size. To emphasize the consequence of this, we have show the mean sizes of clusters in Fig.4 in thick vertical lines. In particular, it can be observed that none of these lines coincide with the maximum of cluster distribution probabilities. However, they help to support the interpretations on the role of water in the considerations below. The principal information they provide is as follows. For 1-octanol, the addition of water diminishes the mean size of the OO clusters while increasing their probabilities (the magenta line in the lower panel is positioned at smaller sizes than the red line), compensated by the increase of the mixed OO_w clusters (the position of the magenta line in the upper panel is similar to that of red line in the lower one). This is in favour of the role of water being a cluster breaker for OO clusters. For 4-octanol, the addition of water also decreases the size of OO clusters, increasing their probability (the pale green line is position at slightly smaller cluster sizes than the dark green line), but this is compensated by a significant increase in mean size of the mixed OO_w clusters. In this case water is more of structure maker.

We now examine the detailed evolution with water inclusion of the 1-octanol cluster distribution in Fig. 5 and that of 4-octanol in Fig. 6. Similar distributions for 2-octanol and 3-octanol are provided in the Supplementary Information document, in Fig.SI-2 and Fig.SI-3. For each octanols, the upper panel shows the cross water-octanol oxygen cluster distribution as function of cluster size, while the lower left and right panels show the octanol oxygen and water oxygen cluster distributions, respectively.

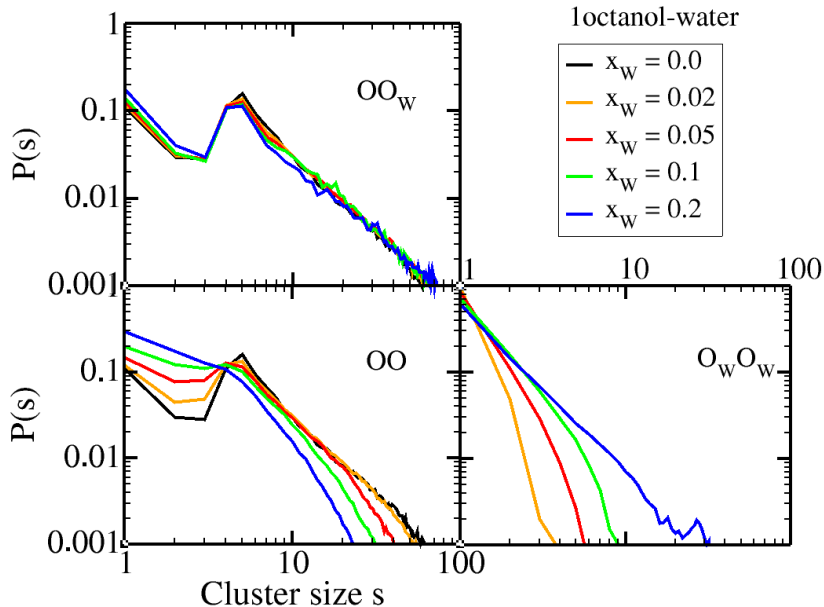


Figure 5: Oxygen atom clusters size distributions for 1-octanol and for different water content.

We first focus on the upper panel of Fig.5, and notice that these cross water-octanol oxygen cluster distribution, for all water concentrations, are nearly identical to their respective pure octanol oxygen distributions (the black curves for $x_w = 0$). The first thing to notice is that all the distributions look more or less alike, and more importantly look like the neat 1-octanol cluster distribution. This is a confirmation that the mixed oxygen clusters are similar to that of neat 1-octanol clusters. Clearly, this implies that the 1-octanol oxygen clusters will be reduced in number and size. This exactly what we observe in the left lower panel: while large OO clusters are in smaller number compared to that of pure 1-octanol, including the cluster-peak region, the number of smaller OO clusters are increased, and in both cases with monotonous trend in water concentration increase. The lower right panel shows water oxygen clusters, which strikes by the fact that there is no cluster peak, just like for pure water [46]. This is partly because water forms globular clusters instead of chain-like ones, since it tends to form tetrahedrally extended space filling patterns, and also because such clusters are more polydispersed.

This analysis clearly demonstrates that water tends to destroy OO clusters, either by inserting into them and breaking them apart, or by breaking them apart into smaller ones. We conclude that water acts as a structure breaker in the case of 1-octanol, since it really breaks the original neat 1-octanol ordering. It is important to note here that by structure breaker we not merely mean to say that water inserts itself in octanol oxygen chains, but that it really make

long OO chains unfavourable.

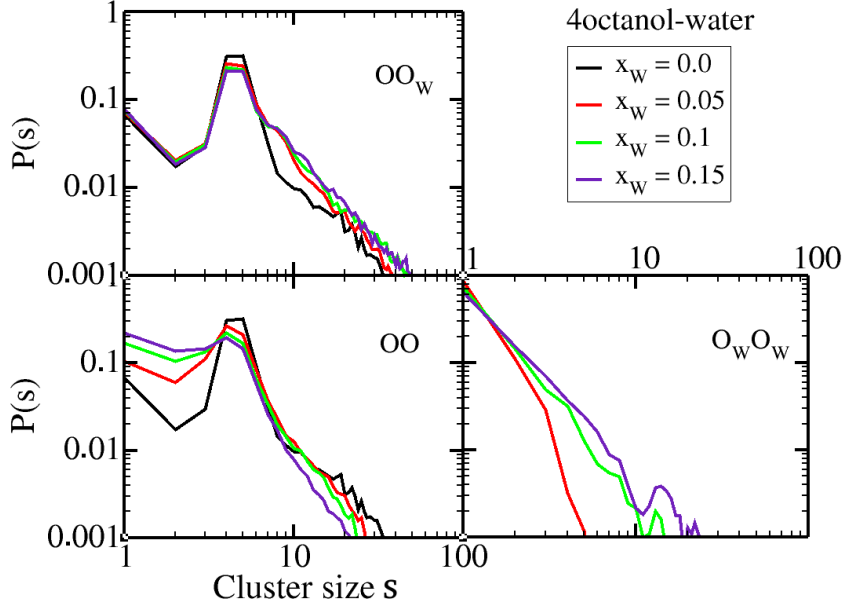


Figure 6: Oxygen atom clusters size distributions for 4-Octanol and for different water content.

This situation changes when branched octanol are concerned. In Fig.6, we see from the upper panel that the mixed OO_w clusters are still more or less similar to that of pure 4-octanol OO clusters (shown in black). We note that the mid range mixed cluster size $7 < s < 11$ tends to be somewhat larger than OO clusters. However, the large OO clusters remain similar to that of neat 4-octanol, as can be seen in the lower left panel. Even though the increase in small OO clusters with water content is similar to that observed in Fig. 5 for 1-octanol (lower left panel), it is really the intermediate/large cluster distribution which is strikingly different. This analysis shows that water acts as structure maker for 4-octanol, in the sense that it preserves the original OO cluster structure, and promotes larger OO_w mixed clusters, a trend also observed for 2-octanol and 3-octanol, as shown in the SI document.

4.2 Correlation functions analysis

In order to rationalize and support most of the interpretations given in the previous discussions, we have examined into some details the various pair correlation functions $g_{a_i b_j}(r)$ and corresponding intermolecular structure factors

$$S_{a_i b_j}(k) = \delta_{ij} + \rho \sqrt{x_i x_j} \int d\mathbf{r} \exp(i\mathbf{k} \cdot \mathbf{r}) [g_{a_i b_j}(r) - 1] \quad (3)$$

where a_i and b_j are atoms types a and b belonging the molecular species i and j , respectively. This structure factor differs from that in Eq.(2) by the absence of the intramolecular correlation term $W_{a_i b_i}(k)$.

Below, we present a comparative analysis of structure functions for 1-octanol and 4-octanol, mostly in the perspective to support the dual role of water. The corresponding data for 2-octanol and 3-octanol can be found in the SI document.

The various oxygen-oxygen pair correlation functions are shown in Figs. 7,9,11, and the corresponding structure factors in Figs. 8, 10, 12. We focus here on comparing the aqueous 1-octanol mixtures with the aqueous 4-octanol mixtures, respectively shown in the right and left panels of the figures. Since the pair correlations are essentially governed by the strong hydrogen bonding interactions, the first peak is unusually high, thus the logarithmic scale has been used. All these figures show features typical of alcohols, with a narrow and high first peak, which witnesses the strong first neighbour correlations due the strong hydrogen binding (represented here by Coulomb interactions), followed by second and higher neighbours depletion correlations, which witness the chaining of the hydroxyl groups. It is these two mechanisms which produce respectively positive and negative contributions to the oxygen-oxygen structure factors, which cancel into forming the pre-peak feature. We note in Figs. 8, 10, 12, that the pre-peak positions correspond to that in the calculated scattering intensities in Fig. 3.

Fig. 7 illustrates the features described above, between two octanol oxygens. In addition, we see that adding water in small concentrations leads to small changes in the correlations for both 1-octanol and 4-octanol, which is the general diminution of correlations. Only the minimum of the depletion well shows marked changes around $r \approx 7.5\text{\AA}$ and $r \approx 6\text{\AA}$ for 1-octanol and 4-octanol, respectively, indicating that water plays its most important role in this distance range, by reducing the depletion. This is in line with the occurrence of small OO chain clusters being favoured, which was found to be common to both octanols through the cluster analysis.

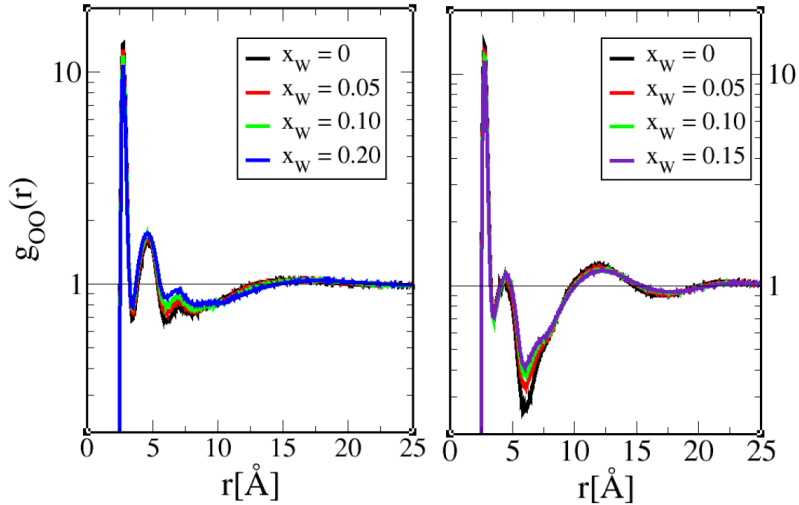


Figure 7: Octanol oxygen-oxygen pair correlation function $g_{OO}(r)$ for 1-octanol (left) and 4-octanol (right), and for various water mole fractions as shown in the legend panels. The pure octanol curves ($x_w = 0$) are presented in black. Note that the vertical scale for the $g_{OO}(r)$ is logarithmic.

In order to gather information about larger clusters, we need to examine the atom-atom structure factors in Fig. 8. Again, we note that there are only little changes in the general shape of these functions with small water addition. Notable features are the marked decrease of the pre-peak amplitude for 4-octanol, as compared to 1-octanol, but also the lesser dependence of overall features with water inclusion for 4-octanol than for 1-octanol, which suggest that OO clusters are not as much affected for 4-octanol than for 1-octanol, except for their numbers, as suggested by the pre-peak amplitude decrease. This is consistent with the cluster analysis results.

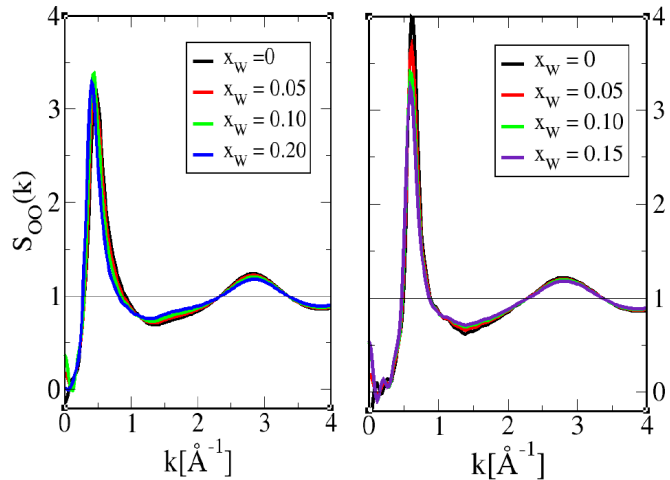


Figure 8: Octanol oxygen-oxygen pair structure factor $S_{OO}(k)$ for 1-octanol (left) and 4-octanol (right), and for various water mole fractions as in Fig.7. The pure octanol curves ($x_W = 0$) are presented in black.

Concerning the mixed OO_W correlations in Fig.9, we note the same features as in Fig.7, namely that the depletion well is the most affected with water addition, as the depletion correlations are decreased. We note however a clear shift of the peak positions at $r \approx 15\text{\AA} - 17\text{\AA}$ for 1-octanol, suggesting the existence of larger mixed clusters with the increase of water content. This is consistent with the cluster analysis about large mixed clusters being more prominent than large OO clusters for wet 1-octanol while in case of wet 4-octanol mixed clusters of average size increase.

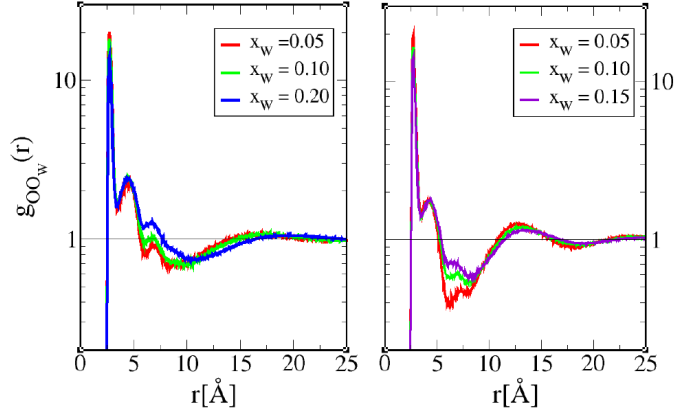


Figure 9: Octanol oxygen - water-oxygen pair correlation function $g_{OO_w}(r)$ for 1-octanol (left) and 4-octanol (right). The lines are as in Fig. 7.

The corresponding structure factors in Fig.10 show much more marked features than in the case of OO correlations. The 1-octanol $S_{OO_w}(k)$ structure factors have a higher pre-peak amplitude than those for 4-octanol, and the changes with water content are more prominent. This is fully consistent with the scenario suggested by the cluster analysis, that mixed oxygen clusters are more abundant in 1-octanol than in 4-octanol, and confirming the intruder role of water in 1-octanol and to a much lesser extent in 4-octanol.

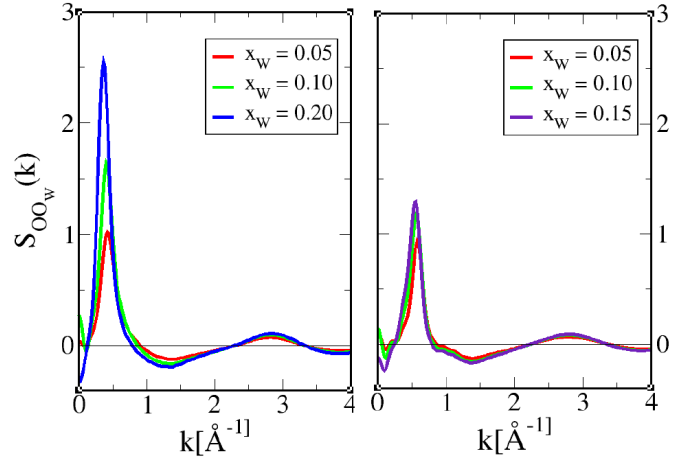


Figure 10: Octanol oxygen - water-oxygen structure factor $S_{OO_w}(k)$ for 1-octanol (left) and 4-octanol (right). The lines are as in Fig. 7.

The water oxygen correlations in Fig.11 and Fig.12 show very peculiar fea-

tures, especially when compared with the corresponding correlations in pure water (black curves). The $g_{O_W O_W}(r)$ clearly suggest the existence of tiny water droplet clusters of 2-3 members, which is witnessed by the fact that the second and third neighbour correlations are well above 1. The large oscillatory features represent droplet-droplet correlations, most probably across alkyl tails, and not within the water-hydroxyl chain clusters. The marked self-water correlations are also consistent with the water cluster analysis not presenting cluster peak.

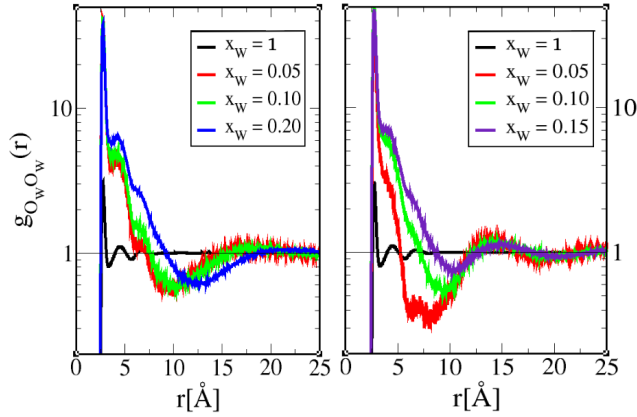


Figure 11: Water-oxygen - water-oxygen pair correlation function $g_{O_W O_W}(r)$ for 1-octanol (left) and 4-octanol (right). The lines are as in Fig. 7, and the pure water correlations are shown in black curves.

The structure factors in Fig.12 tend to confirm the above analysis for $g_{O_W O_W}(r)$. There is a marked pre-peak around $k \approx 0.4 \text{ \AA}^{-1}$, which is in line with that of the octanol pre-peak and x-ray pre-peak, suggesting that water is part of the hydroxyl clusters, and not unexpectedly so. We note also that this pre-peak tends to become a $k = 0$ concentration fluctuation peak in the case of 4-octanol, which is markedly visible for $x_W = 0.15$. This is consistent with the earlier demixing of 4-octanol with water content.

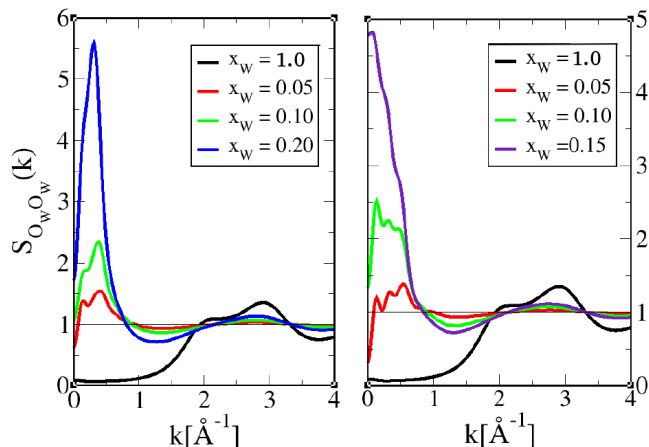


Figure 12: Water-oxygen - water-oxygen structure factors $S_{O_w O_w}(k)$ for 1-octanol (left) and 4-octanol (right). The lines are as in Fig. 7, except that the pure water correlations are shown in black curves.

We note the enormous difference between pure water correlations (black curves) and those for very small water concentrations, suggesting the radical change in microscopic structure. The main peak in $S_{O_w O_w}(k)$ for pure water, which is in fact the shoulder peak around $k \approx 2 \text{ \AA}^{-1}$ (which corresponds to water diameter $\sigma \approx 3 \text{ \AA}$), disappears for the aqueous octanol mixtures, indicating that the bulk water structure does not exist anymore, and is replaced by water aggregated structures.

Similar analysis for 2-octanol and 3-octanol can be made from the figures in the SI document (Fig.SI-4 to Fig.SI-9). Finally, the influence of water in the alkyl tail correlation functions is shown in the SI document, in Fig.SI-10 and Fig.SI-11, for the last carbon atom C_{-8} . It is found that these functions are much less sensitive to water inclusion, which is at first understandable since water does not sit in the alkyl atom areas. However, the dependence on water of 1-octanol is quite visible on the structure factor pre-peak, while that of 4-octanol shows none. This is another indirect proof of water affecting 1-octanol more than it does for the branched 4-octanol.

4.3 Details from snapshots

It is instructive to compare the aggregate structures formed by the hydroxyl groups and water molecules. In Fig.13 we provide such comparison between aqueous 1-octanol (left) and aqueous 4-octanol(right) for a low water content of $x_w = 0.05$, and in Fig.14 for the higher water content $x_w = 0.15$. For the low water content, we observe mostly the differences in chaining of the hydroxyl groups. For 1-octanol the longer chaining is quite apparent, while smaller chains

and also monomers are visible on the right panel for 4-octanol. It is equally seen that small water clusters are part of larger octanol clusters, in both panels.

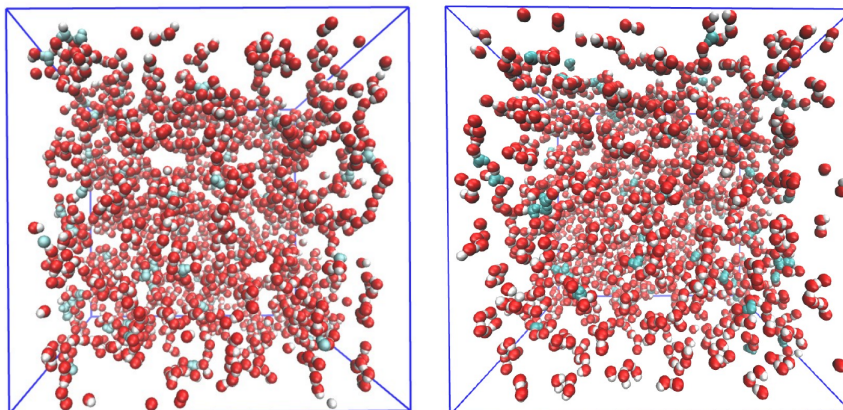


Figure 13: Comparison of snapshots for the $x_w = 0.05$ low water mole fraction, between 1-octanol (left) and 4-octanol (right). Only the hydroxyl groups (oxygen in red and hydrogen in white) and water (in blue) are shown. Snapshots are made with VMD [47].

In Fig.14, for $x_w = 0.15$, we see a marked difference in clustering between 1-octanol and 4-octanol, the latter being more clustered and fewer monomers than for 1-octanol are observed. This is consistent with water increasing the number of chains in 1-octanol (since all of the water is always part of octanol chain clusters), hence with water acting as an *OO* chain breaker (there is a clear illusion of “more” water in the left panel, even the total number of water molecules is the same in both panels).

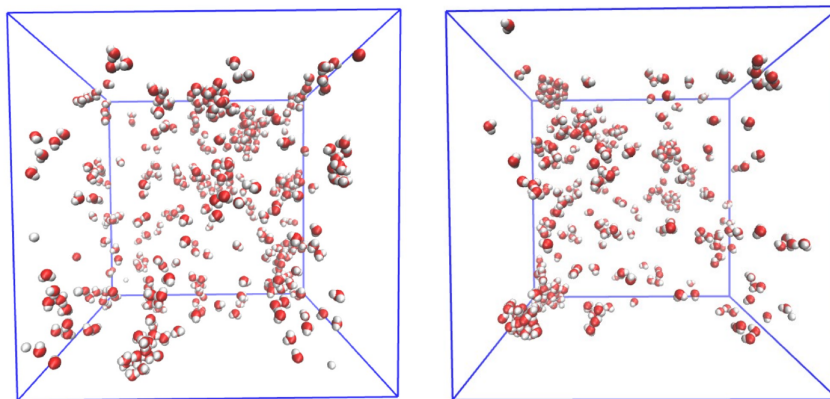


Figure 14: Comparison of snapshots for the $x_w = 0.15$ higher water mole fraction, between 1-octanol (left) and 4-octanol (right). Only the water molecules are shown (oxygen in red and hydrogen in white). Snapshots are made with VMD [47].

5 Discussion and Conclusion

In the present work, we have shown that computer simulations can be used to interpret experimental x-ray spectra of aqueous alcohol n-octanol mixtures in the water poor region, not only by reproducing the changes in shape of the diffraction intensities with water concentrations, but additionally by providing support to the intuitive interpretations of the pre-peak positions and amplitude displacements with water inclusion. More importantly, this study has highlighted the dual role played by water, which depends indirectly on the topology (i.e. branching) of the alkyl tails. It is generally believed that water has a H-bond structure which is so complex that it leads to many of the anomalies found in neat water [48], but also that the nature of different solutes perturb this complex structure, either by destroying or enforcing it. Such solutes are called chaotropes and kosmotropes[49]. Many interesting effects in aqueous mixtures are often described or attributed in terms of this vocabulary[50, 51, 52, 53, 54].

In the present paper, we show that water itself can act as a structure maker/preserver or breaker, depending on the nature of the order in non-aqueous systems, herein the n-octanols. More importantly, this dual role depends on the hydrophobic sub-molecular component of the solute. Since water demixes from long alcohols, it is not surprising that it would act as a structure breaker for 1-octanol. On the other hand, the role of water as structure preserver in the branched octanol is intriguing. It is not the first example of water acting as structure maker, since direct micelle formation is helped by water cooperating in the outer corona region. Similarly, the role of water in biological environment is also believed to play a structuring role. The structural details provided

herein may help better understand the role of water, and pave the way for further investigations.

While the computer simulation study of water rich binary mixtures is plagued with spurious demixing issues in many cases [55, 56, 57, 58, 59, 60], in the present study we demonstrate that this is not the case for water poor mixtures. On contrary, it is apparent that the study provides results very consistent with experimental scattering intensities, indicating that it is not a model issue, as is often formulated when considering problematic water rich simulations [61, 62, 57]. It is quite tempting to deduce that the apparent spurious water segregation and demixing could be a genuine physical effect, in the very short time (less than the microsecond) and small sizes (box sizes below 50 nm). Water may tend to form large segregated domains in a very short period, before a re-entering melting of these domains happens and lead to the final equilibrium mixture. This problem may not be perceptible at experimental level (unless explicitly looked for). From these remarks, it could be interesting to look at water nucleation problems in binary mixtures of aqueous organic molecules from the water rich side. As stated above, the very good agreement observed between the experimental and calculated x-ray scattering intensities, and for very different systems, tend to indicate that subtle self-assembly issues in aqueous poor conditions can be properly studied by model computer simulations.

6 Acknowledgements

We thank DELTA for providing synchrotron radiation at beamline BL2 and technical support. Martina Požar gratefully acknowledges funding of the Croatian Science Foundation under the project no. UIP-2017-05-1863 *Dynamics in Micro-segregated Systems* and the computational resources of the server UniST-Phy at the University of Split. This work was supported by the BMBF via DAAD (PROCOPE 2021-2023, Project-ID: 57560563) within the German-French collaboration PROCOPE (46644XK), *Supra-molecular order in complex liquids: experiment and theory*.

References

- [1] Pierce, W.; MacMillan, D. X-ray studies on liquids: the inner peak for alcohols and acids. *Journal of the American Chemical Society* **1938**. *60*, 779–783.
- [2] Warren, B. X-ray diffraction in long chain liquids. *Phys. Rev.* **1933**. *44*, 969–973.
- [3] Magini, M.; Paschina, G.; Piccaluga, G. On the structure of methyl alcohol at room temperature. *The Journal of Chemical Physics* **1982**. *77*, 2051–2056.

- [4] Narten, A.; Habenschuss, A. Hydrogen bonding in liquid methanol and ethanol determined by x-ray diffraction. *The Journal of Chemical Physics* **1984**. *80*, 3387–3391.
- [5] Sarkar, S.; Joarder, R. N. Molecular clusters and correlations in liquid methanol at room temperature. *The Journal of Chemical Physics* **1993**. *99*, 2032–2039.
- [6] Sahoo, A.; Nath, P.; Bhagat, V.; Krishna, P.; Joarder, R. Effect of temperature on the molecular association in liquid d-methanol using neutron diffraction data. *Physics and Chemistry of Liquids* **2010**. *48*, 546–559.
- [7] Karmakar, A.; Krishna, P.; Joarder, R. On the structure function of liquid alcohols at small wave numbers and signature of hydrogen-bonded clusters in the liquid state. *Physics Letters A* **1999**. *253*, 207–210.
- [8] Sarkar, S.; Joarder, R. N. Molecular clusters in liquid ethanol at room temperature. *The Journal of Chemical Physics* **1994**. *100*, 5118–5122.
- [9] Franks, N. P.; Abraham, M. H.; Lieb, W. R. Molecular organization of liquid n-octanol: An x-ray diffraction analysis. *Journal of Pharmaceutical Sciences* **1993**. *82*, 466–470.
- [10] Vahvaselkä, K. S.; Serimaa, R.; Torkkeli, M. Determination of liquid structures of the primary alcohols methanol, ethanol, 1-propanol, 1-butanol and 1-octanol by x-ray scattering. *Journal of Applied Crystallography* **1995**. *28*, 189–195.
- [11] Sahoo, A.; Sarkar, S.; Bhagat, V.; Joarder, R. N. The probable molecular association in liquid d-1-propanol through neutron diffraction. *The Journal of Physical Chemistry A* **2009**. *113*, 5160–5162.
- [12] Karmakar, A. K.; Sarkar, S.; Joarder, R. N. Molecular clusters in liquid tert-butyl alcohol at room temperature. *The Journal of Physical Chemistry* **1995**. *99*, 16501–16503.
- [13] Tomšič, M.; Jamnik, A.; Fritz-Popovski, G.; Glatter, O.; Vlček, L. Structural properties of pure simple alcohols from ethanol, propanol, butanol, pentanol, to hexanol: Comparing monte carlo simulations with experimental saxs data. *The Journal of Physical Chemistry B* **2007**. *111*, 1738–1751.
- [14] Yamaguchi, T.; Hidaka, K.; Soper, A. The structure of liquid methanol revisited: a neutron diffraction experiment at -80c and +25c. *Molecular Physics* **1999**. *96*, 1159.
- [15] Benmore, C.; Loh, Y. The structure of liquid ethanol: A neutron diffraction and molecular dynamics study. *The Journal of Chemical Physics* **2000**. *112*, 5877–5883.

- [16] Akiyama, I.; Ogawa, M.; Takase, K.; Takamuku, T.; Yamaguchi, T.; Ohtori, N. Liquid structure of 1-propanol by molecular dynamics simulations and x-ray scattering. *Journal of Solution Chemistry* **2004**. *33*, 797–809.
- [17] Sillrén, P.; Swenson, J.; Mattsson, J.; Bowron, D.; Matic, A. The temperature dependent structure of liquid 1-propanol as studied by neutron diffraction and epsr simulations. *The Journal of Chemical Physics* **2013**. *138*, 214501.
- [18] Chen, B.; Siepmann, J. I. Microscopic structure and solvation in dry and wet octanol. *The Journal of Physical Chemistry B* **2006**. *110*, 3555–3563. PMID: 16494411.
- [19] Vrhovšek, A.; Gereben, O.; Jamnik, A.; Pusztai, L. Hydrogen bonding and molecular aggregates in liquid methanol, ethanol, and 1-propanol. *The Journal of Physical Chemistry B* **2011**. *115*, 13473–13488.
- [20] Cerar, J.; Lajovic, A.; Jamnik, A.; Tomšič, M. Performance of various models in structural characterization of n-butanol: Molecular dynamics and x-ray scattering studies. *Journal of Molecular Liquids* **2017**. *229*, 346 – 357.
- [21] Lehtola, J.; Hakala, M.; Hämäläinen, K. Structure of liquid linear alcohols. *The Journal of Physical Chemistry B* **2010**. *114*, 6426–6436.
- [22] Požar, M.; Bolle, J.; Sternemann, C.; Perera, A. On the x-ray scattering pre-peak of linear mono-ols and the related microstructure from computer simulations. *J. Phys. Chem. B* **2020**. *124*, 8358–8371.
- [23] Bolle, J.; Bierwirth, S. P.; Požar, M.; Perera, A.; Paulus, M.; Münzner, P.; Albers, C.; Dogan, S.; Elbers, M.; Sakrowski, R.; et al. Isomeric effects in structure formation and dielectric dynamics of different octanols. *Phys. Chem. Chem. Phys.* **2021**. *23*, 24211–24221.
- [24] Požar, M.; Lovrinčević, B.; Zoranić, L.; Primorac, T.; Sokolić, F.; Perera, A. Micro-heterogeneity versus clustering in binary mixtures of ethanol with water or alkanes. *Physical Chemistry Chemical Physics* **2016**. *18*, 23971.
- [25] Hill, A. E.; Malisoff, W. M. The mutual solubility of liquids. iii. the mutual solubility of phenol and water. iv. the mutual solubility of normal butyl alcohol and water. *Journal of the American Chemical Society* **1926**. *48*, 918–927.
- [26] MacCallum, J. L.; Tieleman, D. P. Structures of neat and hydrated 1-octanol from computer simulations. *Journal of the American Chemical Society* **2002**. *124*, 15085–15093. PMID: 12475354.
- [27] Marcus, Y. Structural aspects of water in 1-octanol. *Journal of Solution Chemistry* **1990**. *19*, 507–517.

- [28] Liltorp, K.; Westh, P.; Koga, Y. Thermodynamic properties of water in the water-poor region of binary water + alcohol mixtures. *Canadian Journal of Chemistry* **2005**. *83*, 420–429.
- [29] Palombo, F.; Tassaing, T.; Paolantoni, M.; Sassi, P.; Morresi, A. Elucidating the association of water in wet 1-octanol from normal to high temperature by near- and mid-infrared spectroscopy. *J. Phys. Chem. B* **2010**. *114*, 9085–9093.
- [30] Sassi, P.; Paolantoni, M.; Cataliotti, R. S.; Palombo, F.; Morresi, A. Water/alcohol mixtures: A spectroscopic study of the water-saturated 1-octanol solution. *J. Phys. Chem. B* **2004**. *108*, 19557–19565.
- [31] Napoleon, R. L.; Moore, P. B. Structural characterization of interfacial n-octanol and 3-octanol using molecular dynamic simulations. *J. Phys. Chem. B* **2006**. *110*, 3666–3673.
- [32] Dargasz, M.; Bolle, J.; Faulstich, A.; Schneider, E.; Kowalski, M.; Sternermann, C.; Savelkouls, J.; Murphy, B.; Paulus, M. X-ray scattering at beamline bl2 of delta: Studies of lysozyme-lysozyme interaction in heavy water and structure formation in 1-hexanol. *Journal of Physics: Conference Series* **2022**. *2380*, 012031.
- [33] Hammersley, A. P.; Svensson, S. O.; Hanfland, M.; Fitch, A. N.; Hausermann, D. Two-dimensional detector software: From real detector to idealised image or two-theta scan. *High Pressure Research* **1996**. *14*, 235–248.
- [34] Pronk, S.; Páll, S.; Schulz, R.; Larsson, P.; Bjelkmar, P.; Apostolov, R.; Shirts, M.; Smith, J.; Kasson, P.; van der Spoel, D.; et al. Gromacs 4.5: a high-throughput and highly parallel open source molecular simulation toolkit. *Bioinformatics* **2013**. *29*, 845–854.
- [35] Martínez, J.; Martínez, L. Packing optimization for automated generation of complex system’s initial configurations for molecular dynamics and docking. *Journal of Computational Chemistry* **2003**. *24*, 819.
- [36] Bussi, G.; Donadio, D.; Parrinello, M. Canonical sampling through velocity rescaling. *The Journal of Chemical Physics* **2007**. *126*, 014101.
- [37] Parrinello, M.; Rahman, A. Crystal structure and pair potentials: A molecular-dynamics study. *Physical Review Letters* **1980**. *45*, 1196.
- [38] Parrinello, M.; Rahman, A. Polymorphic transitions in single crystals: A new molecular dynamics method. *Journal of Applied Physics* **1981**. *52*, 7182.
- [39] Hockney, R. *Methods in computational physics, vol. 9*, Orlando Academic Press, vol. 9, chap. The potential calculation and some applications, 135–221. **1970**.

- [40] Darden, T.; York, D.; Pedersen, L. Particle mesh ewald: An nlog(n) method for ewald sums in large systems. *The Journal of Chemical Physics* **1993**. *98*, 10089.
- [41] Hess, B.; Bekker, H.; Berendsen, H.; Fraaije, J. Lincs: A linear constraint solver for molecular simulations. *Journal of Computational Chemistry* **1997**. *18*, 1463.
- [42] Jorgensen, W. Optimized intermolecular potential functions for liquid alcohols. *The Journal of Physical Chemistry* **1986**. *90*, 1276.
- [43] Berendsen, H. J. C.; Grigera, J. R.; Straatsma, T. P. The missing term in effective pair potentials. *The Journal of Physical Chemistry* **1987**. *91*, 6269–6271.
- [44] Debye, P. Zerstreung von röntgenstrahlen. *Annalen der Physik* **1915**. *351*, 809–823.
- [45] Debye, P. Scattering of x-rays. In *The collected papers of Peter J.W. Debye*, Interscience Publishers. **1954**.
- [46] Zoranić, L.; Sokolić, F.; Perera, A. Microstructure of neat alcohols: A molecular dynamics study. *The Journal of Chemical Physics* **2007**. *127*, 024502.
- [47] Humphrey, W.; Dalke, A.; Schulten, K. Vmd: Visual molecular dynamics. *Journal of Molecular Graphics* **1996**. *14*, 33–38.
- [48] Chaplin, M. water structure and science.
- [49] Ball, P.; Hallsworth, J. E. Water structure and chaotropy: their uses, abuses and biological implications. *Phys. Chem. Chem. Phys.* **2015**. *17*, 8297–8305.
- [50] Collins, K. D.; Neilson, G. W.; Enderby, J. E. Ions in water: Characterizing the forces that control chemical processes and biological structure. *Biophysical Chemistry* **2007**. *128*, 95–104.
- [51] Hribar, B.; Southall, N. T.; Vlachy, V.; Dill, K. A. How ions affect the structure of water. *Journal of the American Chemical Society* **2002**. *124*, 12302–12311.
- [52] Marcus, Y. Effect of ions on the structure of water: Structure making and breaking. *Chemical Reviews* **2009**. *109*, 1346–1370.
- [53] Laurent, H.; Soper, A. K.; Dougan, L. Trimethylamine n-oxide (tmao) resists the compression of water structure by magnesium perchlorate: terrestrial kosmotrope vs. martian chaotrope. *Phys. Chem. Chem. Phys.* **2020**. *22*, 4924–4937.

- [54] Vraneš, M.; Tot, A.; Papović, S.; Panić, J.; Gadžurić, S. Is choline kosmotrope or chaotrope? *The Journal of Chemical Thermodynamics* **2018**. *124*, 65–73.
- [55] Perera, A.; Sokolić, F. Modeling nonionic aqueous solutions: The acetone-water mixture. *The Journal of Chemical Physics* **2004**. *121*, 11272.
- [56] Kežić, B.; Perera, A. Revisiting aqueous-acetone mixtures through the concept of molecular emulsions. *The Journal of Chemical Physics* **2012**. *137*, 134502.
- [57] Lee, M.; van der Vegt, N. A new force field for atomistic simulations of aqueous tertiary butanol solutions. *The Journal of Chemical Physics* **2005**. *122*, 114509.
- [58] Gupta, R.; Patey, G. N. Aggregation in dilute aqueous tert-butyl alcohol solutions: Insights from large-scale simulations. *The Journal of Chemical Physics* **2012**. *137*, 034509.
- [59] Overduin, S. D.; Perera, A.; Patey, G. N. Structural behavior of aqueous t-butanol solutions from large-scale molecular dynamics simulations. *The Journal of Chemical Physics* **2019**. *150*, 184504.
- [60] Banerjee, S.; Furtado, J.; Bagchi, B. Fluctuating micro-heterogeneity in water-tert-butyl alcohol mixtures and lambda-type divergence of the mean cluster size with phase transition-like multiple anomalies. *The Journal of Chemical Physics* **2014**. *140*, 194502.
- [61] Chitra, R.; Smith, P. E. A comparison of the properties of 2,2,2-trifluoroethanol and 2,2,2-trifluoroethanol/water mixtures using different force fields. *The Journal of Chemical Physics* **2001**. *115*, 5521–5530.
- [62] Overduin, S. D.; Patey, G. N. Comparison of simulation and experimental results for a model aqueous tert-butanol solution. *The Journal of Chemical Physics* **2017**. *147*, 024503.